 DOI: 10.1002/masy.200951109

Gas-Phase Polymerization with Transition Metal Catalysts Supported on Montmorillonite – A Particle Morphological Study

Sang-Young A. Shin,[1] *Leonardo C. Simon,*[*1] *João B. P. Soares,*[*1] *Günter Scholz,*[2] *Timothy F. L. McKenna*[3]

Summary: This investigation focuses on the mechanism of particle fragmentation and growth when clay-supported metallocene catalysts are used to polymerize ethylene in gas-phase reactors. We supported bis(cyclopentadienyl)-zirconium dichloride (Cp_2ZrCl_2) on montmorillonite (MMT) pretreated with triisobutylaluminum and 10-undecence-1-ol to produce in-situ polyethylene-clay nanocomposites. During gas phase polymerization, the MMT layers were exfoliated by the growing polymer chains, starting from the openings of the clay galleries. After microtoming, the cross-section of the fragmented MMT particles showed bundles of distorted silicate layer stacks, proving that exfoliation took place during polymerization, producing an in-situ polyethylene-clay nanocomposite. Calculations of d-spacing by transmission electron microscopy (TEM) matched those measured by X-ray diffraction (XRD) analysis.

Keywords: clay; gas-phase polymerization; montmorillonite; metallocene catalysts; nanocomposites; polyethylene

Introduction

When supported transition metal catalysts are used for polymerization, the final polymer particle replicates the shape of the support when the polymerization and supporting conditions are favorable. Investigations on particle morphology, particle growth and fragmentation have been approached experimentally and theoretically, as discussed in recent reviews.[1–3]

Many different types of inorganic carriers have been tested as supports for metallocene catalysts.[2,4–7] The most frequently investigated supports are spherical silica and polymeric particles.[8–14] Generally, spherical silica particles lead to good polymer particle morphology and have been widely employed.

One of the supporting techniques commonly described in literature is to impregnate the catalyst on a MAO-treated silica support.[13] Although this method has been investigated by a number of research groups in slurry or gas-phase polymerization reactors, the use of clay-supported catalysts for gas-phase polymerization have been seldom reported,[14] even though this is a very attractive procedure to produce polyolefin-clay nanocomposites.

In this paper, a novel approach to prepare in-situ polyolefin nanocomposites in gas-phase reactors using catalysts supported on montmorillonite (MMT) is described. The catalyst is supported inside the MMT galleries. In-situ polymerization allows the layered structure of MMT particles to be exfoliated directly in the reactor during the polymerization. Because polymerization is carried out in gas-phase, there is no solvent in the system to extract

[1] Department of Chemical Engineering, University of Waterloo, Waterloo, ON, Canada N2L 3G1
E-mail: jsoares@uwaterloo.ca
[2] Department of Physics, University of Waterloo, Waterloo, ON, Canada, N2L 3G1
[3] Department of Chemical Engineering, Queen's University, Kingston, ON, Canada K7L 3N6

the catalyst sites (Cp_2ZrCl_2) from the MMT surface. The present study focuses on understanding the mechanism of particle morphology formation and particle growth using scanning (SEM) and transmission (TEM) electron microscopy.

Experimental Part

Materials

Commercial MMT (M-KSF) was purchased from Aldrich and used after the washing and drying steps described in our previous publication.[15] The catalyst, bis(cyclopentadienyl)-zirconium dichloride (Cp_2ZrCl_2) was purchased from Aldrich. Triisobutyl aluminum (TIBA), ($Al(C_3H_7)_3$, 1.9 mol/L solution in toluene), methylalumoxane (MAO), 10-undecence-1-ol (UOH), and monochlorobenzene were purchased from Aldrich Co. and used without further purification. Ethylene and nitrogen were supplied by PRAXAIR Products, Inc.

Catalyst Preparation

The pre-contacting of MMT with Cp_2ZrCl_2 was carried out at room temperature ($23 \pm 2\,^{\circ}C$) in a 250-mL glass reactor equipped with a stirrer. Dried MMT (1 g) was first treated with TIBA and UOH in toluene solution (MMT/TIBA/UOH), followed by addition of a solution containing the transition metal catalyst. The solvent was evaporated under vacuum for 3 hours at room temperature until a free flowing powder was obtained. The supported catalyst was transferred to a glass vial (5 mL) and soaked with 0.2 g of MAO (10 wt.-% MAO in toluene) at room temperature in a glove box before polymerization.

Pre-Polymerization

Pre-polymerizations were carried out under mild conditions (room temperature and atmospheric pressure) without stirring, using a 5-mL glass vial, located inside a 250-mL Schlenk tube. Before the pre-polymerization, the Schlenk tube was purged 3 times with with ethylene. Two polymerization times, 3 and 24 hours, were used for the study of MMT particle fragmentation under mild polymerization conditions.

Gas-Phase Polymerization in a High-Pressure Autoclave

For high pressure gas-phase polymerizations, a turbo-sphere reactor equipped with gas purification, temperature control, and data acquisition devices was used.[16,17] One hundred grams of NaCl was used as a seed bed and TMA was used to scavenge impurities. For all the polymerization runs, the residual TMA was removed from the reactor prior to catalyst injection by evacuation or successive dilution with ultra-high purified N_2 and venting after the impurity scavenging stage.

Polymerization was carried out under constant stirring by pressurizing the reactor with ethylene after injection of the pre-polymerized catalyst particles. Catalyst activities were calculated from the ethylene flow rates measured with a mass flow meter. After 1 hour, the polymerization was quenched by adding methanol and stirred for additional 10 minutes. The polymer particles, with NaCl, were transfer to a 1-L beaker, filled with acidic ethanol, and then filtered with a filter paper. After being washed with 30 mL of acidic ethanol 3 times, the polymer particles were finally dried at 78 °C for 24 hours under vacuum to obtain the polyethylene-MMT nanocomposites.

Characterization

X-Ray diffraction (XRD) patterns for wide angle ($4 \sim 65\ 2\theta$ degree) were recorded on a Simens-500 diffractometer. The beam was Cu Kα radiation ($\lambda = 0.154$ nm) operated, at 40 kV and 30 mA in transmission mode. The basal spacing of MMT before and after intercalation was estimated from the position of (d100) peak in the XRD pattern. XRD for small angle ($0 \sim 10\ 2\theta$ degree) was D8-ADVANCE powder X-ray diffractometer operating at 40 kV and 30 mA, which was made in BRUKER AXS, INC.

The nanocomposite morphology was examined by high resolution transmission electron microscopy (TEM) using a Philips CM-20 Super Twin unit (200 kV, resolution 0.24 nm), operating at an acceleration voltage of 80 KV. The specimens were sliced in a liquid nitrogen chamber with a diamond knife (LEICA EM UC6). The thickness of the specimens was 50–80 nm. The morphology was also investigated with a scanning electron microscope (SEM) (LEO 1530, LEO Electron Microscopy, Ltd.). MMT was analyzed as received to identify the particle size and its distribution in the polymer matrices. The powder was place over a double-face adhesive conductive tape on top of an aluminum stub. The sample was then gold-coated for 5 minutes to produce a film of gold approximately 15–20 nm on the sample surface. The polymer fluff obtained after polymerization was prepared as nanocomposite specimens. The small specimens were glued onto the aluminum stubs. Before SEM observation, the dry samples were painted with 15–20 nm thick gold for electron conduction. The pressure in the vacuum chamber for SEM analysis was approximately 2.5×10^{-6} mBar, and the electron gun current was 10 kV.

The spectra in transmission mode in Fourier transform infrared (FT-IR) spectroscopy were recorded in the range from 400 to 4000 cm^{-1}, after 32 scans, with resolution of 4 cm^{-1}. Calibration of the wavenumber was automatically done by the instrument using an internal polystyrene film. Spectra reported here were subtracted from a background spectrum obtained with no sample.

Results and Discussion

Stirring was not used during pre-polymerization because we wanted to observe changes in particle morphology without the interference of outer mechanical forces. Particle morphology after 3 hours of polymerization is shown in Figure 1.a. Hereafter this sample will be called 3HP (3HP stands for 3 hours of pre-polymerization). Three different types of particles are observed in Figure 1.a: ***A*** – barely polymerized surface, ***B*** – polymer on MMT surface without cracks or fragmentation, and ***C*** – MMT platelets fragmented into smaller particles. Figure 1.b shows a TEM image of intercalated MMT particles. The different contrast levels observed in Figure 1.b represent stacked MMT particles, the darker regions representing higher staking levels. During in-situ polymerization, aggregates of MMT primary particles are first separated into smaller particles by the growing polymer. Each primary particle consists of several layers with a distance of 27 nm between the platelets, as can be inferred from Figure 1.b. Each intercalated plate has a thickness of approximately 5 nm, and appears to be bent at the edges.

In a second set of experiments, the pre-polymerization was allowed to proceed for 24 hours. These samples will be called 24HP. They are compared to the 3HP samples with the same degree of magnification (2K,

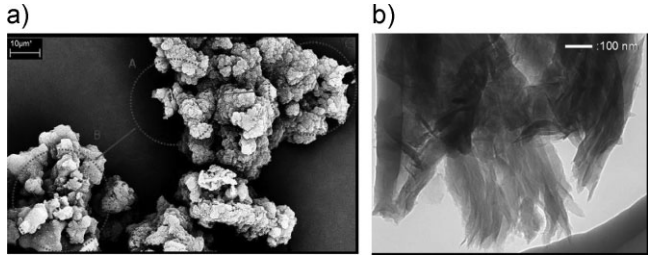

Figure 1.
MMT particle morphology after 3 hours of pre-polymerization (3HP): (a) SEM image, (b) TEM image of an 80 nm thin film, prepared with ultra microtoming under −160 °C in a cryo-chamber.

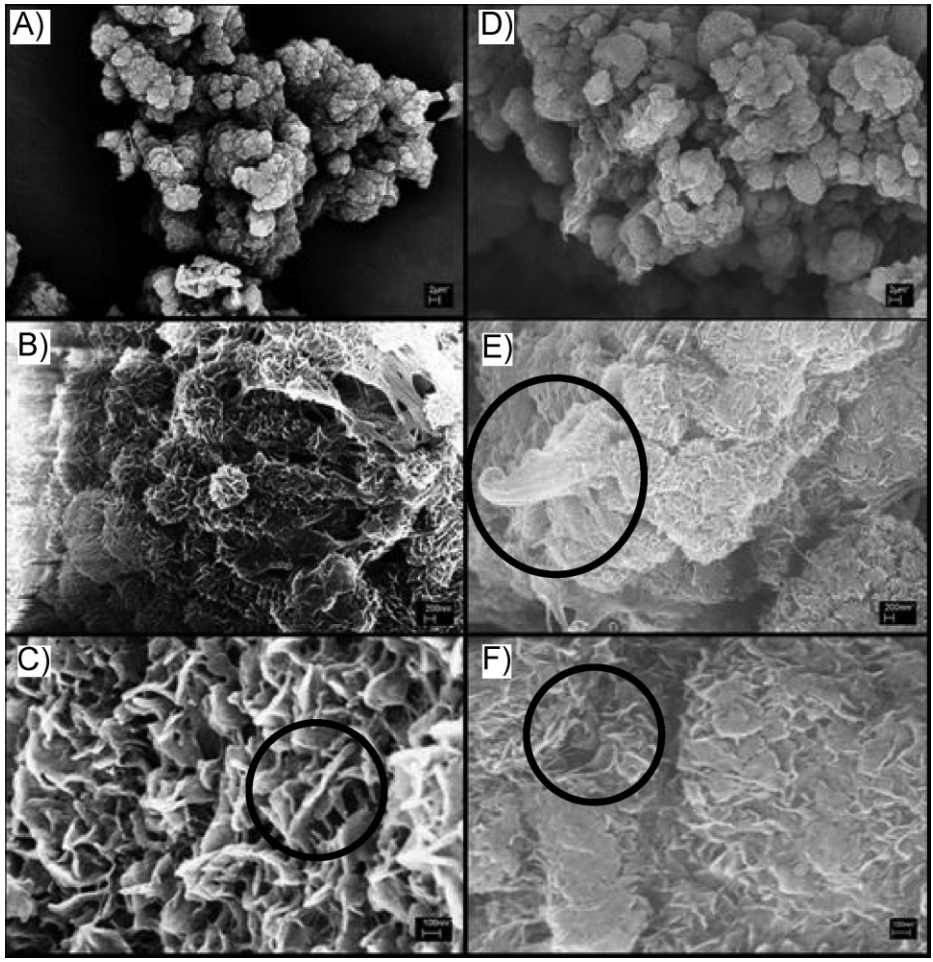

Figure 2.
Comparison of particle morphologies after 3 hours (***A***, ***B***, ***C***) and 24 hours (***D***, ***E***, ***F***) of polymerization.

30K and 100K) in Figure 2. Inspection of the micrographs shows that the pre-polymerization induced the fragmentation of the MMT particles after 3 hours (***A***, ***B*** and ***C***) and further encapsulation by polymer after 24 hours (***D***, ***E*** and ***F***).

In micrograph ***B***, MMT has been fragmented in particles of about 10 μm diameter and 100 nm polymer projections are observed on the surface of the MMT platelets, whereas in micrograph ***E***, the presence of 1 μm polymer threads are observed. It is likely that these polymer threads grew from inside the particles during polymerization. Other researchers have described the formation of polymer threads or fibrils on the catalyst support during early stages of polymerization with Ziegler-Natta catalysts.[18] Polyethylene fibres were also reported in the polymerization with a metallocene catalyst supported on MCM-41 particles at low temperature.[19] At the largest magnification (30K times, scale bar of 200 nm), the surface morphology of 3HP and 24HP particles are clearly different. The 3HP particles shows polymer projections on their surface (micrograph ***C***), whilst the 24HP particles present curved platelets on fragmented surfaces (micrograph ***F***) with

polymer threads that are approximately 1 μm (micrograph ***E***), probably coming from inside the MMT particles. As the polymerization proceeds, it is reasonable to assume that the continuous production of polymer inside and around the MMT particles leads to the accumulation of polymer and further fragmentation. The polymer accumulation around the tactoids is responsible for fragmentation of the MMT particles and the polymer accumulation inside the clay galleries is responsible for the exfoliation of the MMT layers.

Selected polymer particles obtained in the pre-polymerization step were microtomed and studied with TEM and XRD to better understand the mechanism of particle growth and fragmentation. Figure 3.a shows the TEM image of a section of a pre-polymerized 24HP particle already shown in Figure 2 (micrographs ***D*** to ***F***). It seems that the exfoliation of the MMT sheets starts from the edges of the clay layers, due to the growth and accumulation of polymer chains between the layers. Figure 3.b shows that the clay platelets of the same sample are well aligned. The distance of 12.5 layers was measured to be 15.5 nm and the d-spacing was calculated as 12.4 Å, which is equivalent to a XRD peak at $2\theta = 7.2^{\circ}$. This indicates that the structure of some MMT particles after the polymerization remains very close to that of the original MMT. The XRD for pristine MMT, and 3HP and 24HP particles, show a d-spacing peak at approximately 7.5°, corresponding to an interlayer distance of 12.3 Å. This XRD data matches well the calculation based on the TEM image shown in Figure 3.b. It seems that, during the gas-phase pre-polymerization, polymer intercalation or exfoliation starts from the edges of the MMT particles, but the core of some of the MMT particles are not substantially exfoliated during polymerization.

Figure 4 shows the diffractograms of pure MMT and 3HP and 24HP nanocomposites. The peaks located at around 21° and 24°correspond to the diffraction planes (110) and (200) of the unit cell of polyethylene crystal. Their intensities increase as the polymer weight percent in the polymerized particles increase from MMT < 3HP < 24HP. The combined evidence of SEM and TEM images, together with XRD patterns, demonstrates that polymerization in the gas-phase starts on the surface of MMT particles, and further induces particle fragmentation.

The morphology of polymer particles made in the high pressure gas-phase reactor was different from the morphology observed after the low pressure pre-polymerization. SEM images in Figure 5

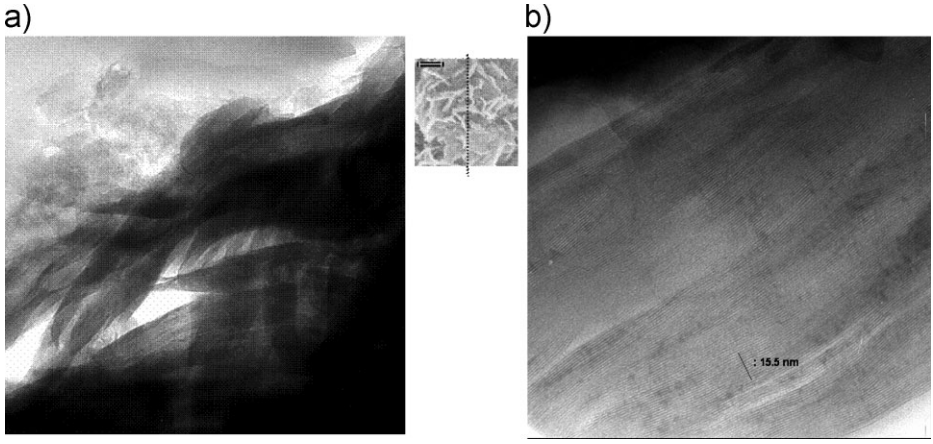

Figure 3.
TEM pictures of a microtomed 24HP particle: (a) the inner edge of the particle after microtoming, showing that the MMT platelets were exfoliated and curved, (b) MMT layered platelets.

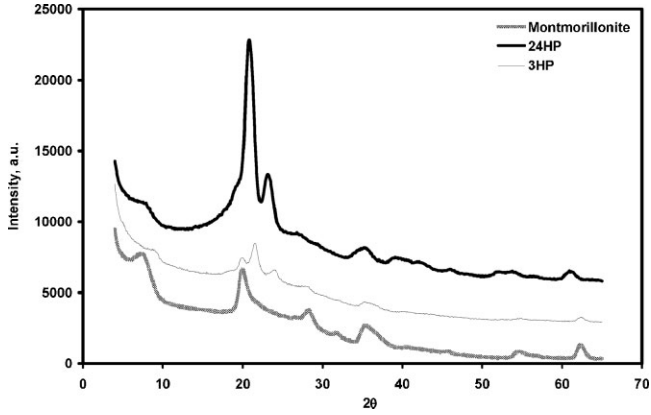

Figure 4.
X-ray diffractograms of pure MMT, 3HP (45 wt.-% MMT) and 24HP (20 wt.-%) nanocomposites.

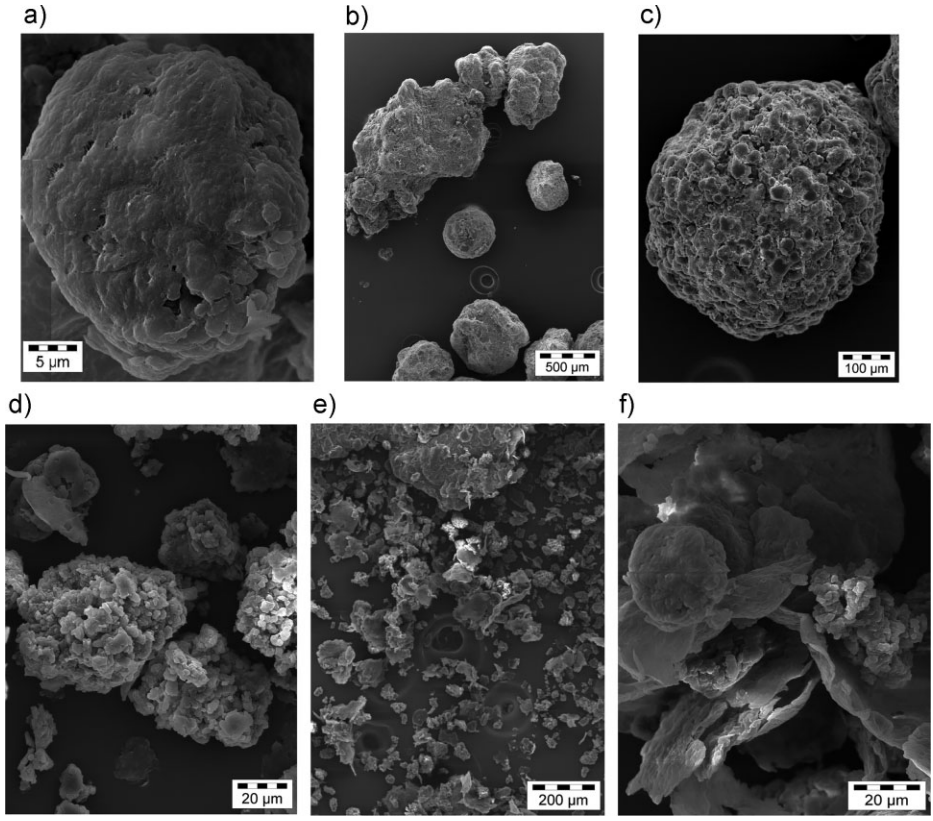

Figure 5.
Morphology of polymer particles after gas-phase polymerization: (a) Expanded image of a particle with polymer outer shell, (b) Several types of particle morphologies, (c) Expanded image of a spherical type particle, (d) Particles without polymer outer shell, (e) Overall morphology, (f) Particles with and without polymer outer shells.

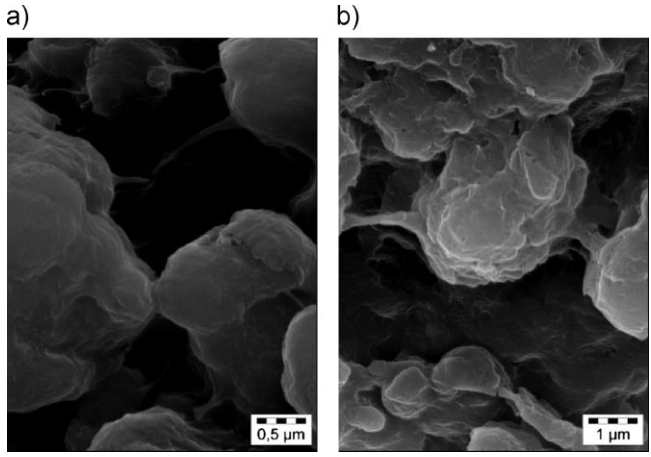

Figure 6.
Morphology of particles after gas-phase polymerization: (a) Attached particles just after fragmentation within particle clusters, (b) Divided particles after fragmentation continued within particle clusters.

show some spherical particles covered by a polymer outer shell and some particles with bare surfaces. The diameter of spherical particles varies from 20 μm to 300 μm (Figure 5.a to 5.c). Fragmented sub-particles were observed with dimension of a few micrometers in Figures 5.d to 5.f. The particle fragmentation observed here seem to follow that proposed in the multigrain model, which has been developed to describe the fragmentation mechanism of magnesium-supported Ziegler-Natta catalysts.[3] The projection, or fibril, morphology described above for pre-polymerization was not observed in polymer particles made under high pressure polymerization.

Figure 6 shows the intraparticle morphology at higher magnifications. In Figure 6.a, some particles seem to be kept attached during the fragmentation, whereas Figure 6.b shows that some particles are linked by polymer threads.

Figure 7 depicts the catalyst activity profile for the gas-phase polymerization

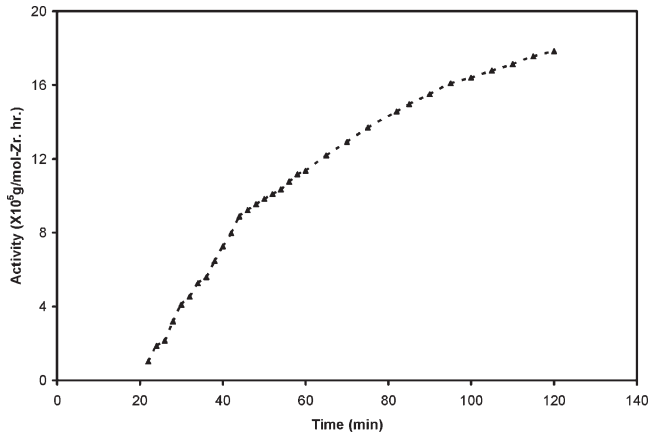

Figure 7.
Activity profile of 24HP samples as a function of polymerization time. Ethylene pressure = 6 bar, polymerization temperature = 73 °C, Al/Zr = 2000.

(sample 24HP). An unexpected induction period was observed during the first 20 minutes of polymerization. The reason for this induction period is not totally clear. It may be caused by reactor over-pressure during catalyst injection or by side reactions between the supported catalyst and TMA used as impurity scavenger. It could also be related to mass transfer limitation during ethylene diffusion from the gas phase to the pre-polymerized catalyst. After the induction period, the polymerization rate increased steadily as the ethylene concentration between the MMT platelets increased during the polymerization. The fragmentation process of the particles could make monomer more accessible to the active sites by increasing surface area and decreasing the characteristic monomer diffusion length. The induction period is followed by a steady growth in activity (acceleration-type kinetics). This type of behaviour is not observed when ethylene is polymerized with unsupported Cp_2ZrCl_2 and is clearly related to the clay fragmentation mechanism in this system.

According to the multigrain model mechanism, a mechanically strong catalyst support that does not fragment easily during polymerization will not favor an increase in surface area. Hence, there will be a mass transfer limitation for monomer diffusion to the active sites that will decrease the catalyst activity and lower the polymerization yield.

The topological structure of alkyl chains inside the MMT galleries has been studied using transmission FT-IR and XRD.[20] The polymer chains are thought to extend either parallel to the clay layers, forming lateral mono- or bi-layers, or radiate away from the surface, forming extended (paraffin-type) mono- or bimolecular arrangements.[21–23] Figure 8 shows the FT-IR spectra ($1400\,cm^{-1}$–$1520\,cm^{-1}$) for 3HP and 24HP pre-polymers, and polyethylene. The CH_2 bending mode, $\delta(CH_2)$, is located, between 1460 and $1474\,cm^{-1}$. While the $\delta(CH_2)$ band for 3HP pre-polymer ranged between $1460\,cm^{-1}$ and $1474\,cm^{-1}$, the $\delta(CH_2)$ band for the pre-polymer 24HP was shifted to a lower frequency range ($1457\,cm^{-1}$–$1473\,cm^{-1}$) and became broader. In the case of polyethylene, the band is located in the lower frequency range ($1467\,cm^{-1}$–$1454\,cm^{-1}$). This type of change is normally associated with more disordered polymer chains (lower trans/gauche conformation ratio). This indicates

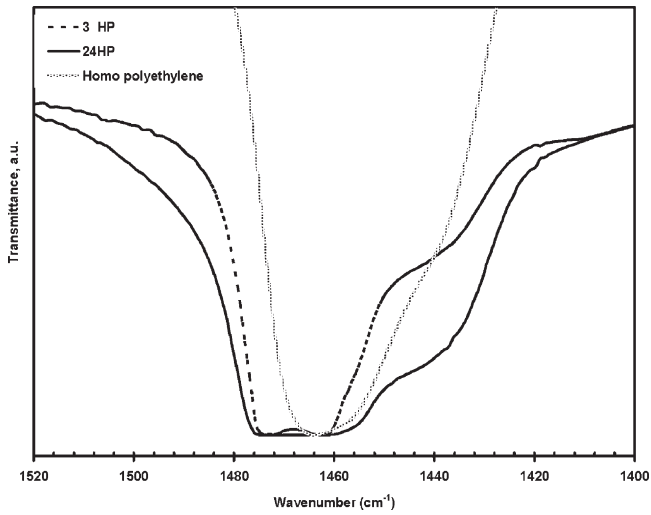

Figure 8.
FT-IR transmittance spectra for 3HP and 24HP pre-polymers and polyethylene displaying different methylene modes. The spectra were obtained at room temperature.

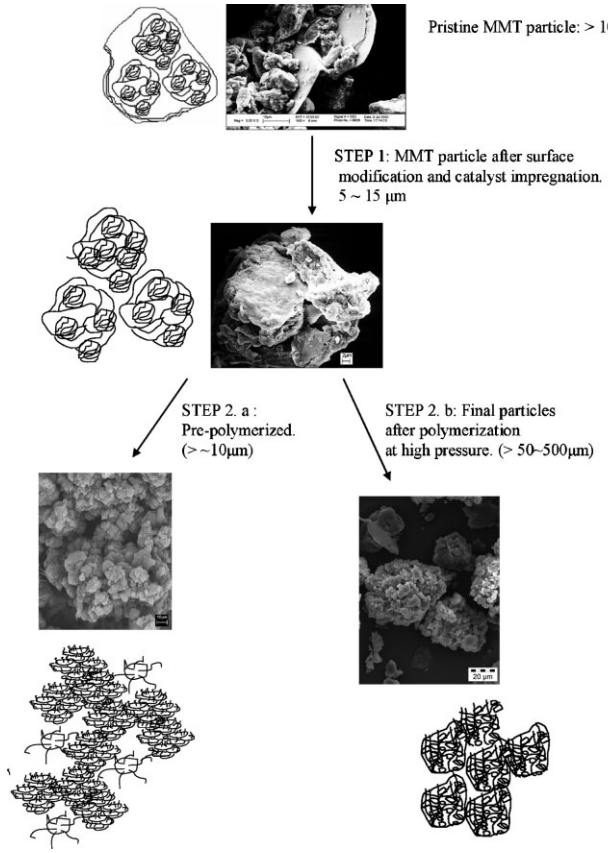

Figure 9.
Proposed mechanism for particle fragmentation with MMT/TIBA/UOH/Cp_2ZrCl_2.

that, as pre-polymerization proceeds from 3 to 24 hours, the polymer chains favor a more disordered configuration due to the tendency of the chains to maximize their conformational entropy.

In Figure 9 we propose an overall particle fragmentation mechanism for MMT-supported catalysts. During the polymerization, polymer chains grow on the surface of MMT particles, around the tactoids, and inside the galleries, establishing the onset of intercalation and exfoliation. The MMT particles are also fragmented into the smaller particles, possibly into clusters of tactoids. Finally, polymer particles with good morphology (free flowing powder with spherical shape particles) are formed during the high-pressure polymerization stage.

Conclusions

Through this morphological and kinetic study of ethylene gas phase polymerization with a MMT-supported catalyst, it can be concluded that MMT fragments due to polymer growth in the early stages of polymerization, and intercalation and exfoliation occurs only to some extent. These conclusions are supported by XRD, SEM and TEM analyses.

Ethylene polymerization with MMT/TIBA/UOH/Cp_2ZrCl_2 had a long induction time, lower activity, and acceleration-type kinetics. Ethylene mass transfer resistances may explain, at least in part, some of these polymerization kinetics characteristics.

A tentative mechanism for particle fragmentation during pre-polymerization

and high pressure ethylene polymerization was also proposed.

[1] J. B. P. Soares, A. E. Hamielec, *Polym. React. Eng.* **1995**, *3*, 261.
[2] G. G. Hlatky, *Chem. Rev.* **2000**, *100*, 1347.
[3] T. F. McKenna, J. B. P. Soares, *Chem. Eng. Sci.* **2001**, *56*, 3931.
[4] J. Janiak, B. Rieger, *Angew. Makromol. Chem.* **1994**, *215*, 47.
[5] T. Kitagawa, T. Uozumi, K. Soga, T. Takata, *Polymer*, **1997**, *38*, 615.
[6] G. Fink, R. Mulhaupt, H. H. Brintzinger, *Ziegler Catalysts, Recent Scientific Innovations and Technological Improvements*, Springer Verlag, Berlin (1st ed.), **1995**, pp. 363.
[7] S. C. Houg, H. T. Ban, N. Kishi, J. Jim, T. Uozumi, K. Soga, *Macromol. Chem. Phys.* **1998**, *199*, 1393.
[8] X. Cheng, O. W. Lofthus, P. A. Deck, P.A., *J. Mol. Catal. A: Chem.* **2004**, *212*, 121.
[9] B. Jongsomjit, P. Praserthdam, P. Kaewkrajang, *Mat. Chem. Phys.* **2004**, *86*, 243.
[10] K. Soga, T. Arai, B. H. Hoang, T. Uozumi, *Macromol. Rapid Commun.* **1995**, *16*, 905.
[11] M. K. Lee, I. B. Kim, C. S. Chin, *J. Organometal. Chem.* **1985**, *290*, 115.
[12] B. Rieger, C. Janiak, *Angew. Makromol. Chem.* **1996**, *215*, 45.
[13] W. Kaminsky, F. Renner, *Makromol. Chem., Rapid Commun.* **1993**, *14*, 239.
[14] C. Liu, T. Tang, B. Huang, *J. Catal.* **2004**, *221*, 162.
[15] S. Y. A. Shin, L. C. Simon, J. B. P. Soares, S. G. Scholz, *Polymer* **2003**, *44*, 5317.
[16] P. Kittilsen, T. F. McKenna, *J. Appl. Polym. Sci.* **2001**, *82*, 1047.
[17] C. Brun, R. Pelletier, *Process for Polymerization in a Gaseous Phase Using Heterogeneous Catalysis and a Spherical Reactor for Carrying Out the Process* US Pat. 4,467,080, (1984).
[18] J. Boor, Ziegler-Natta Catalysts and Polymerizations, Academic Press, New York **1979**, pp. 202.
[19] Z. Ye, S. Zhu, W. J. Wang, H. AlSyouri, Y. S. Lin, *J. Pol. Sci., Part B, Pol. Phys.* **2003**, *41*, 2433.
[20] R. A. Vaia, R. K. Teukolsky, E. P. Giannelis, *Chem. Mater.* **1994**, *6*, 1017.
[21] G. Lagaly, *Clay Miner.* **1979**, *27*, 1.
[22] G. Lagaly, K. Beneke, A. Weiss, *Am. Miner.* **1975**, *60*, 650.
[23] A. Weiss, *Angew. Chem. Inter. Ed.* **1963**, *2*, 134.

